Communication

Using MoS$_2$/Fe$_3$O$_4$ as Ion-Electron Transduction Layer to Manufacture All-Solid-State Ion-Selective Electrode for Determination of Serum Potassium

Yan Su [1], Ting Liu [1], Caiqiao Song [1], Aiqiao Fan [1], Nan Zhu [2], Bingbing Sun [1] and Cheng Yang [1,*]

[1] State Key Laboratory of Fine Chemicals, Department of Chemistry, School of Chemical Engineering, Dalian University of Technology, Dalian 116024, China; susu@dlut.edu.cn (Y.S.); liuting123@mail.dlut.edu.cn (T.L.); songcq0127@163.com (C.S.); aiqiaofan@mail.dlut.edu.cn (A.F.); bingbingsun@dlut.edu.cn (B.S.)

[2] Zhang Dayu School of Chemistry, Dalian University of Technology, Dalian 116024, China; nanzhu@dlut.edu.cn

[*] Correspondence: yangcheng@dlut.edu.cn

Abstract: As an essential electrolyte for the human body, the potassium ion (K$^+$) plays many physiological roles in living cells, so the rapid and accurate determination of serum K$^+$ is of great significance. In this work, we developed a solid-contact ion-selective electrode (SC-ISE) using MoS$_2$/Fe$_3$O$_4$ composites as the ion-to-electron transducer to determine serum K$^+$. The potential response measurement of MoS$_2$/Fe$_3$O$_4$/K$^+$-ISE shows a Nernst response by a slope of 55.2 ± 0.1 mV/decade and a low detection limit of 6.3×10^{-6} M. The proposed electrode exhibits outstanding resistance to the interference of O$_2$, CO$_2$, light, and water layer formation. Remarkably, it also presents a high performance in potential reproducibility and long-term stability.

Keywords: ion-selective electrode; solid contact layer; MoS$_2$/Fe$_3$O$_4$ composites; serum potassium

1. Introduction

Potassium (K$^+$) is an essential element in the human body. The normal range for potassium level in the blood is 3.5 to 5.5 mM. K$^+$ takes part in the metabolism and many physiological activities in the human body, such as maintaining acid-base balance, the normal functions of nerves and muscles, and even cardiac pacing [1]. Abnormal K$^+$ concentration is a symptom of several diseases, including kidney diseases, alcoholism, anorexia, heart disease, diabetes, Addison's disease [2,3]. In the modern medical community, potassium level is considered one of the most vital indicators for electrolyte detection, especially for the rescue of critically ill patients [4]. The standard methods for detection of K$^+$ concentration include gravimetry, ion chromatography, flame photometry, atomic absorption spectrometry, and the ion-selective electrode method [5,6]. A blood gas analyzer based on the liquid-contact ion-selective electrode (LC-ISE) is applied to determine the serum K$^+$ in clinical testing. However, LC-ISE has inner filling solutions, which leads to unfavourable storage and miniaturization [7,8].

The all-solid-state ion-selective electrode using solid-contact layer, termed solid-contact ISE (SC-ISE), does not require inner filling solutions and shows an excellent potential for portable serum K$^+$ detection [9–11]. Cattrall et al. [12] developed the original solid-state ion-selective electrode, in which the ion-selective membrane (ISM) coats onto a metallic conductor directly. However, the primary reason hindering the widespread application and conventional analysis of ISE is the unstable response to the electrode potential. This limitation is mainly due to the effective ion-to-electron conversion between the ISM (ion conduction) and the substrate electrode (electronic conduction) [13,14]. Therefore, to overcome this limitation, an intermediate layer is designed and proposed to facilitate the ion-to-electron transduction, thus contributing to the further development

of the SC-ISEs [15,16]. During the past decades, various SC functional materials have been incorporated into SC-ISEs as ion-to-electron transducers, particularly conductive polymers [9,17]. However, some SC-ISEs with conductive polymers as the SC layer are affected by the water layers and the interference of light, O_2, and CO_2 [18,19]. In contrast, nanostructured materials, such as noble metal nanomaterials, carbon nanotubes, graphene, and hybrid composites, exhibit excellent physicochemical properties [20–23]. According to two theories of the ion–electron transfer between the SC and ISM, the SC layer plays a vital role in stabilizing the interfacial potential. Meanwhile, its presence not only enlarges double-layer capacitance but also activates redox activity [24]. Therefore, it requires a high specific surface area and outstanding redox activity of composites as SC to achieve a stable electrode potential [16,17,24].

Dichalcogenides have two-dimensional (2D) structures similar to graphene. These graphene-like materials are characterized by a large effective surface area, as well as excellent mechanical and electronic properties [25]. These properties are consistent with the transducing layer materials we require. MoS_2 is a typical layered transition metal dichalcogenide widely used in supercapacitors, transistors, catalysts, and other fields [26]. Qin et al. [19] fabricated a K^+-ISE with 3D MoS_2 nanoflowers as an SC layer, which shows a good performance in electrochemical measurements. Although the MoS_2 nanoflowers as an SC layer present excellent properties, it cannot be ignored that there is ample space between the petals of the MoS_2 nanoflowers, making their structure relatively fragile. However, the spaces can be effectively supported by filling with ultrafine nanoparticles to prevent the spatial structure of the MoS_2 nanoflowers from collapsing.

Meanwhile, we aim to further increase the redox capacitance of the SC layer by loading redox active nanomaterials. Magnetite (Fe_3O_4) is considered as a promising candidate. Some studies have shown that the specific capacitance of Fe_3O_4 nanoparticles hybridized with reduced graphene oxide (rGO) is much higher than those of pure Fe_3O_4 and Fe_3O_4/CNTs composites [27,28]. Moreover, the large specific surface area provided by ultrafine particles leads to higher ion fluxes, and the transport distance in the ultrafine particles is shorter, which can significantly improve the ion–electron conversion [29,30]. Therefore, filling MoS_2 nanoflowers with Fe_3O_4 nanoparticles may support the resulting structure and avoid its collapse. Meanwhile, it is also effective in improving the capacitance of the SC layer. In addition, MoS_2 nanoflowers are built with a layered structure to disperse Fe_3O_4 nanoparticles, thus improving their electrochemical properties effectively.

In this work, a stable K^+-ISE was facilely manufactured with MoS_2/Fe_3O_4 nanocomposites as ion-to-electron transducers. Subsequently, the electrochemical measurements of the self-made electrode were investigated to evaluate their potential reproducibility, stability, water layer, and anti-interference performance. Finally, the electrode was successfully applied to detect the actual serum K^+ in real samples.

2. Materials and Methods

2.1. Synthesis of the MoS₂/Fe₃O₄ Composites

The MoS_2 nanoflowers were synthesized through the hydrothermal method [26]. Typically, 1.06 g ammonium molybdate (($NH_4)_6Mo_7O_{24}$·$4H_2O$) and 1.96 g thiourea (CH_4N_2S) were added in 30 mL ultrapure water, and they are mixed. After stirring for 30 min, the mixture turned into a uniform and stable blue solution. Subsequently, the solution was poured into the reactor, and the reactor was placed in an oven at 180 °C for 24 h. After the reactor was completely cooled, the precipitated products were obtained by filtration, and the products were washed with ultrapure water and dried under reduced pressure conditions for 12 h. In the end, white MoS_2 nanoflowers were obtained.

The MoS_2/Fe_3O_4 composite was synthesized through the solvothermal method [31]. A combination of 0.10 g of the MoS_2 nanoflowers, 0.25 g $FeCl_3$·$6H_2O$, 30 mL ethanol, and 5 mL ultrapure water was mixed by ultrasonic treatment for 2 h. Then, 0.75 g NaOAc was added to the solution. After stirring for 1 h, the mixture was poured into the reactor at 200 °C for 24 h. After the process, the black product (MoS_2/Fe_3O_4) was separated by

magnetic force and washed with ultrapure water. Finally, the MoS_2/Fe_3O_4 composites were obtained after being dried in the vacuum oven for 12 h.

2.2. Fabrication of All-Solid-State Potassium Selective Electrodes

The glass-carbon disk electrode (GC, i.d. 3 mm) was polished with alumina powder (1.0, 0.3, and 0.05 μm) and then rinsed with ethanol and ultrapure water. To prepare the SC layer, the MoS_2/Fe_3O_4 composites were dissolved in water, then mixed evenly under ultrasonic treatment. Additionally, 5-μL MoS_2/Fe_3O_4 suspensions were then coated onto the GC electrode and dried in air. The above steps were repeated four times.

The composition of the membrane solution was 131.2 mg o–NPOE, 2.0 mg valinomycin, 1.2 mg NaTFPB, and 65.6 mg PVC, which was dissolved in 1.6 mL THF [32]. For the K^+-ISE fabrication, 20 μL of the membrane solution was dripped onto the top of the GC electrode modified by the MoS_2/Fe_3O_4 transducer and left to dry naturally. This procedure was repeated 5 times. The prepared K^+-ISE was conditioned in 1 mM KCl for more than 24 h before being used [19].

2.3. Electrochemical Measurements

The open-circuit potential measurement was performed with a CHI660B Electro-Chemical workstation (Shanghai Chenhua Apparatus Corporation, Shanghai, China) with two-electrode systems. Double liquid junction Hg/Hg_2Cl_2 was used as the reference electrode, and 1 M LiOAc was used as a salt bridge electrolyte. With 10 mL ultrapure water as the base solution, 50 μL of standard potassium ion solution with different concentrations was added per 100 s. Both electrochemical impedance spectroscopy (EIS) and chronopotentiometry tests were performed with a three-electrode system in 0.1 M KCl. The working electrode was the modified electrode, the auxiliary electrode was a platinum wire, and Ag/AgCl (3 M KCl) was used as the reference electrode. The EIS measurements were performed in the frequency range from 10^5 Hz to 10^{-2} Hz with an excitation amplitude of 20 mV with a Zahner electrochemical workstation in the case of open-circuit voltage. A chronopotentiometry test was recorded using a CHI660B electrochemical workstation. A constant current of +1 nA was applied on the working electrode for 60 s, followed by a current of −1 nA for 60 s.

3. Results and Discussion

3.1. Characterization of the Synthesized MoS_2/Fe_3O_4 Composites

To determine the morphology and composition evolution, scanning electron microscope (SEM; S-4800, Hitachi, Tokyo, Japan), transmission electron microscopy (TEM; G2 F30 S-Twin, Hillsboro, USA), and X-ray diffraction (XRD; Rigaku smartlab 9, Tokyo, Japan) were employed. As shown in Figure 1a, MoS_2 presents as 3D nanoflowers, which are aggregated by many nanoflakes. Such construction implies increasing the surface area, facilitating effective interfacial contact between the ISM and GC electrode. In Figure 1b, it can be noted that the petals of the MoS_2 nanoflowers are decorated with many nanoparticles. Another TEM image shows that the Fe_3O_4 nanoparticles are selectively generated along the edge of the MoS_2 nanoflakes, as shown in Figure 1c. The MoS_2 and MoS_2/Fe_3O_4 were characterized by XRD, as shown in Figure 1d. Compared with pure MoS_2 whose characteristic diffraction peaks appear at 13°, 32.9°, and 58°, we also observed a series of diffraction peaks at 31.2°, 35.6°, 43°, and 57.7° in the spectrum of the MoS_2/Fe_3O_4 composites, which demonstrated the successful deposition of Fe_3O_4 on MoS_2 [29]. Thus, the composites with a high specific surface area decorated with the redox activity of nanoparticles were successfully synthesized.
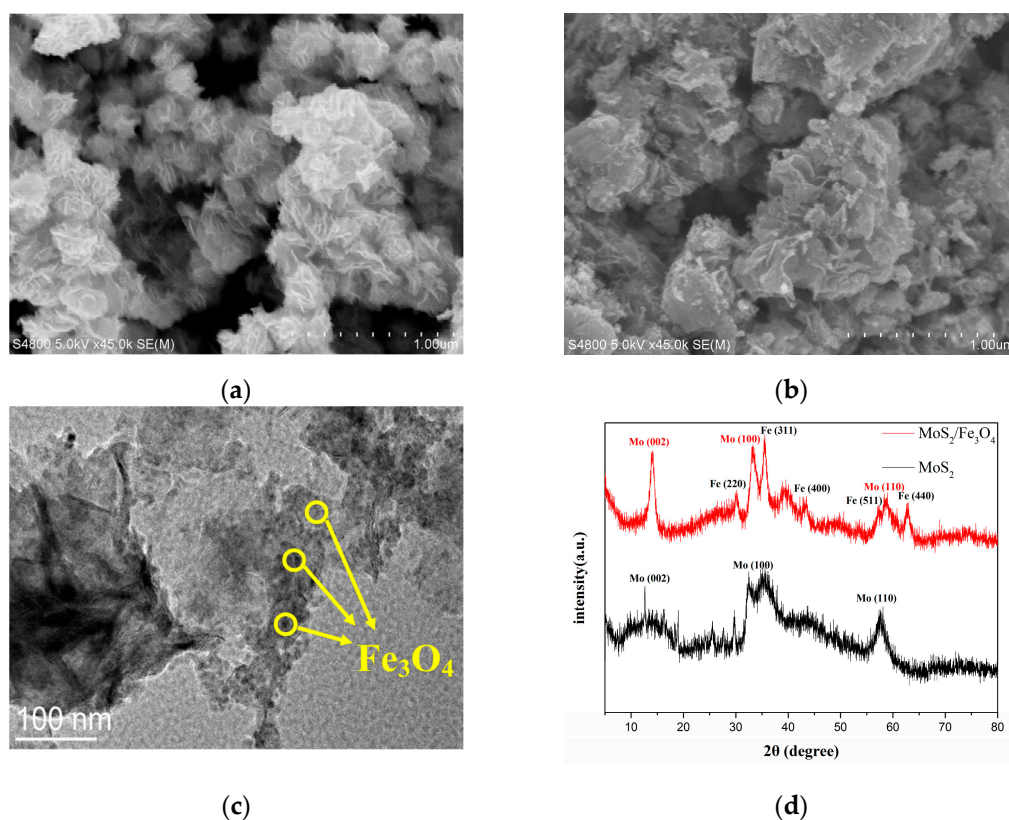
Figure 1. (**a**) SEM image of MoS_2; (**b**) SEM, (**c**) TEM, and (**d**) XRD images of MoS_2/Fe_3O_4 composites.

3.2. Potassium Response Test

With the MoS_2/Fe_3O_4 composites as the SC layer, the potentiometric electromotive force (EMF) was applied to measure the potential response of $GC/MoS_2/Fe_3O_4/K^+$-ISE. The dynamic potential response of the electrode at different K^+ concentrations and the corresponding calibration curve are shown in Figure 2. The fabricated electrode shows a Nernst response with a slope of 55.2 ± 0.1 mV/decade with an activity range from 10^{-5} M to 10^{-2} M and a detection limit of 6.3×10^{-6} M. Activity coefficients were calculated according to a two-parameter Debye–Hückel approximation.
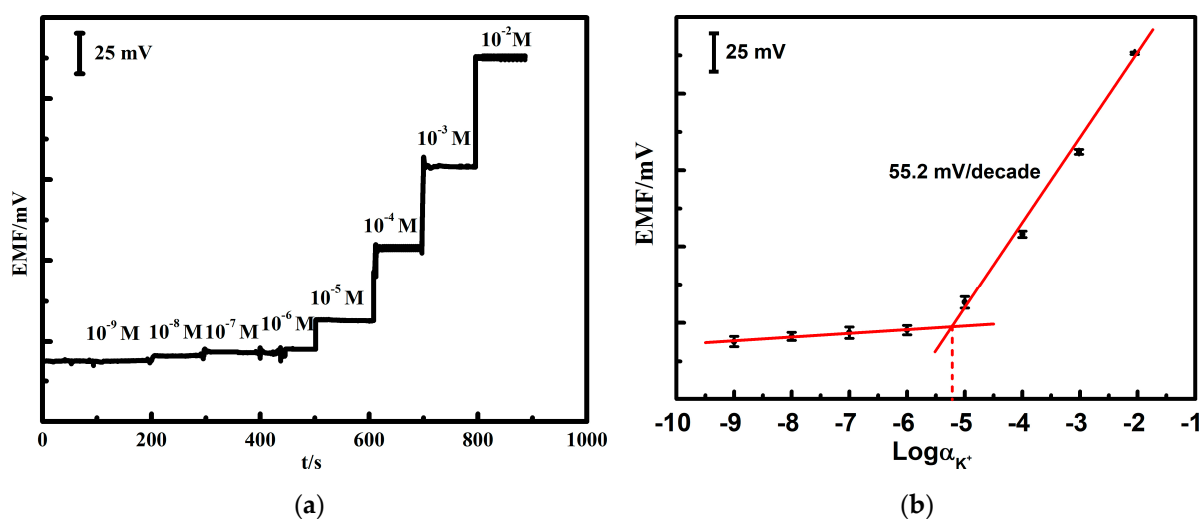

Figure 2. (**a**) Open-circuit potential responses of different K^+ concentrations; (**b**) calibration curve of $GC/MoS_2/Fe_3O_4/K^+$-ISE.

3.3. Electrochemical Impedance and Chronopotentiometry Test

Electrochemical impedance spectroscopy was performed to verify the electrical characterization of the $GC/MoS_2/Fe_3O_4/K^+$-ISE. As shown in Figure 3a, the high-frequency semicircle represents the bulk resistance of ISM and the contact resistance between the ISM and the underlying conductor.
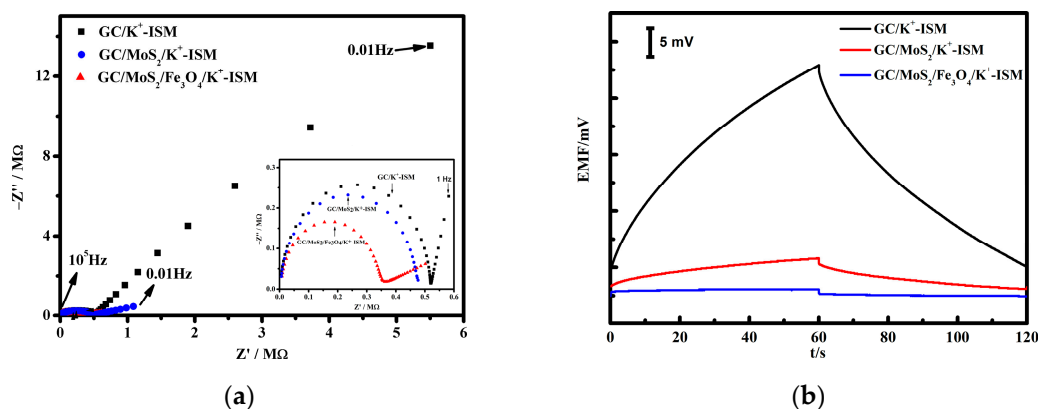

Figure 3. (**a**) Impedance spectra (inset: impedance spectrum in the high-frequency region); (**b**) current reversal chronopotentiometry test of GC/K^+-ISE, $GC/MoS_2/K^+$-ISE, and $GC/MoS_2/Fe_3O_4/K^+$-ISE in 0.1 M KCl.

The resistance of $GC/MoS_2/Fe_3O_4/K^+$-ISE was about 0.36 MΩ, which is smaller than that of $GC/MoS_2/K^+$-ISE (0.47 MΩ) and GC/K^+-ISE (0.52 MΩ). These can be explained by the fact that the MoS_2/Fe_3O_4 layer may reduce the charge transition resistance across the interference [33]. In addition, the $GC/MoS_2/Fe_3O_4/K^+$-ISE exhibited a smaller semicircle in the low-frequency region, which indicates that the electrode has a smaller transfer impedance and a larger capacitance at the "blocked" interface [16].

Chronopotentiometry was performed to monitor the potential stability of the modified electrode. As shown in Figure 3b, when the current is reversed, the potential jump occurs because of the membrane resistance [24]. The resistance of $GC/MoS_2/Fe_3O_4/K^+$-ISE was calculated as 0.40 MΩ, which is consistent with the electrochemical impedance spectroscopy studies. In addition, potential drift can be applied for evaluating the material suitability for the SC layer [33]. The potential drifts of the $GC/MoS_2/Fe_3O_4/K^+$-ISE, $GC/MoS_2/K^+$-ISE, and GC/K^+-ISE were 2.9, 60.0, and 457.1 μV/s, respectively. Notably, the potential drift rate for $GC/MoS_2/Fe_3O_4/K^+$-ISE was much smaller than other electrodes, thus showing the excellent potential stability of the $GC/MoS_2/Fe_3O_4/K^+$-ISE. According to the equation of $\Delta E/\Delta t = I/C$, the corresponding capacitance values were 350.0, 16.7, and 2.2 μF, respectively. MoS_2/Fe_3O_4 composites have the feature of high capacitance, which can significantly accelerate the ion–electron transition, thus enhancing the potential stability of the sensor [33]. Moreover, it is comparable to other earlier presented SC layers, such as conducting polymers [34], carbon-based materials [35], Ag@AgCl/TMMCl [36], and MoS_2 nanoflowers [19].

3.4. Anti-Interference and Water Layer Test

Light, O_2, and CO_2 will cause potential drifts, undesirable for the SC-ISE. Therefore, some experiments were performed to investigate the influence of these factors on $GC/MoS_2/Fe_3O_4/K^+$-ISE. As shown in Figure 4a, the self-made electrode merely shows a slightly positive potential drift. The results show that the SC layer of MoS_2/Fe_3O_4 composites can effectively prevent the interference of light, O_2, and CO_2.
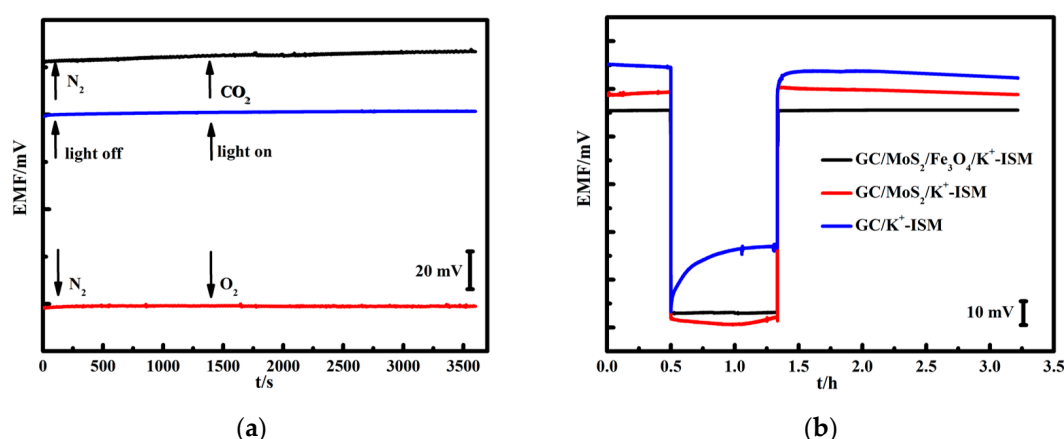
Figure 4. (**a**) Light, O_2, and CO_2 interference tests of GC/MoS$_2$/Fe$_3$O$_4$/K$^+$-ISE in 0.1 M KCl. (**b**) Water layer tests of GC/K$^+$-ISE, GC/MoS$_2$ /K$^+$-ISE, and GC/MoS$_2$/Fe$_3$O$_4$/K$^+$-ISE.

Since the fabricated electrode must soak in the aqueous solution before being used and during detection, this may contribute to forming a water layer between the ISM and the SC layer. The water layer interference test was conducted concerning the work of Pretsch et al. [37]. As shown in Figure 4b, by switching the electrode with the transduction layer from the KCl solution to the NaCl solution, no significant change of potential was observed. In contrast, the electrode without the transduction layer has a significant positive shift. Furthermore, when they are put into the solution containing K$^+$ again, only GC/K$^+$-ISE shows an apparent negative potential drift. The above results indicate the absence of a water layer in the electrodes with the transduction layer. Consequently, the electrode with MoS$_2$/Fe$_3$O$_4$ composites as the SC layer can be successfully used in an aqueous solution.

3.5. Potential Reproducibility and Stability Test

The potential reproducibility and long-term stability are important indexes to evaluate the characteristics of the SC layer [33]. Therefore, a K$^+$ response test was repeated six times under different K$^+$ concentrations to investigate the potential reproducibility of GC/MoS$_2$/Fe$_3$O$_4$/K$^+$-ISE. As shown in Figure 5a, the relative standard deviation of the potential value for each solution is within 2.8% in the range from 1.0×10^{-5} to 1.0×10^{-2} M, implying excellent reproducibility of this SC-ISE. Additionally, the long-term stability of the GC/MoS$_2$/Fe$_3$O$_4$/K$^+$-ISE was performed by measuring the EMF on different dates and with the same SC-ISE (Figure 5b). The Nernst slope of the electrode response and detection limit has no apparent changes for 15 days, indicating that the self-made GC/MoS$_2$/Fe$_3$O$_4$/K$^+$-ISE has good long-term potential stability.
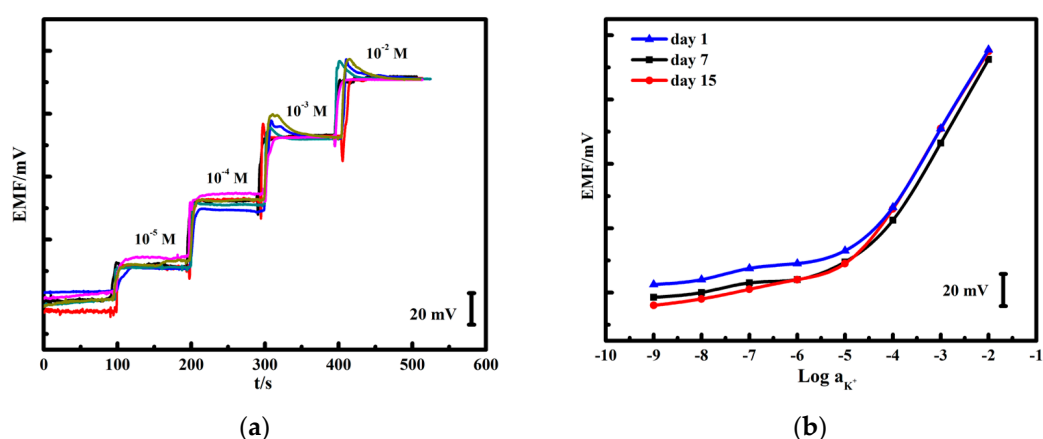

Figure 5. (**a**) Time-dependent potential response trace of the GC/MoS$_2$/Fe$_3$O$_4$/K$^+$-ISE for 6 times. (**b**) Calibration curve of the GC/MoS$_2$/Fe$_3$O$_4$/K$^+$-ISE on different days.

3.6. Analytical Applications

To verify the practical potential of our method in a clinical measurement, the electrode is used to detect the concentration of K^+ in a 5-mL serum sample. It is observed that the electrode presents a response of 511.9 ± 1.0 mV with a calculated concentration of 6.14 ± 0.24 mM (n = 6), which is highly accordant with the results obtained from the standard atomic absorption spectrometry 6.41 ± 0.18 mM with an RSD of 2.8% (n = 6). The relative deviation between these two methods is 4.2%, indicating that the proposed $GC/MoS_2/Fe_3O_4/K^+$-ISE is a promising tool for detecting serum K^+ concentrations. However, it should be pointed out that because of the large size of the electrode, the required serum for this method is still large. In our future research, we will focus on the miniaturization of the size of the electrode to speed up the practical popularization progress.

4. Conclusions

In this paper, MoS_2/Fe_3O_4 composites were introduced as an ion-to-electron transducer material in SC-ISE. The fabricated $GC/MoS_2/Fe_3O_4/K^+$-ISE shows a good Nernst response with a slope of 55.2 mV/decade within the activity range from 1.0×10^{-5} to 1.0×10^{-2} M. The potential drift of the $GC/MoS_2/Fe_3O_4/K^+$-ISE was only 2.9 μV/s, and the capacitance value was 350.0 μF, which contributes to the potential stability of this SC-ISE. Notably, the electrode exhibited excellent resistance to interference from O_2, CO_2, light, and water layer formation. It also presented a high performance in potential reproducibility with the RSD within 2.8% (n = 6) and long-term stability for 15 days. Furthermore, in contrast with the atomic absorption method, the electrode allows for the accurate and quick detection of K^+ in serum with an RSD of 4.8%. Finally, we can conclude that the proposed SC-ISE based on MoS_2/Fe_3O_4 composites as an ion–electron transduction layer would have a good application prospect in the clinical determination of serum K^+. In the future, we will further realize the miniaturization of SC-ISEs through screen-printed electrode technology.

Author Contributions: Y.S.: Investigation, Writing, Project administration. T.L.: Methodology, Validation, Investigation, Writing. C.S.: Methodology, Validation, Investigation, Reviewing the manuscript. A.F.: Investigation, Validation, Writing. N.Z.: Methodology, Validation, Writing. B.S.: Methodology, Validation, Writing. C.Y.: Conceptualization, Methodology, Writing, Supervision, Project administration, Funding acquisition. All authors have read and agreed to the published version of the manuscript.

Institutional Review Board Statement: Not applicable.

Informed Consent Statement: Not applicable.

Data Availability Statement: Not applicable.

Conflicts of Interest: The authors declare no conflict of interest.

References

1. Dixon, D.L.; Abbate, A. Potassium levels in acute myocardial infarction: Definitely worth paying attention to. *Eur. Heart J. Cardiovasc. Pharmacother.* **2015**, *1*, 252–253. [CrossRef]
2. Su, H.; Ruan, W.; Ye, S.; Liu, Y.; Sui, H.; Li, Z.; Sun, X.; He, C.; Zhao, B. Detection of physiological potassium ions level in human serum by Raman scattering spectroscopy. *Talanta* **2016**, *161*, 743–747. [CrossRef]
3. Ahmed, A.; Zannad, F.; Love, T.E.; Tallaj, J.; Gheorghiade, M.; Ekundayo, O.J.; Pitt, B. A propensity-matched study of the association of low serum potassium levels and mortality in chronic heart failure. *Eur. Heart J.* **2007**, *28*, 1334–1343. [CrossRef] [PubMed]

4. Shlomai, G.; Berkovitch, A.; Pinchevski-Kadir, S.; Bornstein, G.; Leibowitz, A.; Goldenberg, I.; Grossman, E. The association between normal-range admission potassium levels in Israeli patients with acute coronary syndrome and early and late outcomes. *Medicine* **2016**, *95*, e3778. [CrossRef] [PubMed]

5. Verdian-Doghaei, A.; Housaindokht, M.R.; Abnous, K. A fluorescent aptasensor for potassium ion detection-based triple-helix molecular switch. *Anal. Biochem.* **2014**, *466*, 72–75. [CrossRef]

6. Tounsi, M.; Braiek, M.B.; Barhoumi, H.; Baraket, A.; Lee, M.; Zine, N.; Maaref, A.; Errachid, A. A novel EIS field effect structures coated with TESUD-PPy-PVC-dibromoaza helicene matrix for potassium ions detection. *Mater. Sci. Eng. C Mater.* **2016**, *61*, 608–615. [CrossRef]

7. Anderson, E.L.; Chopade, S.A.; Spindler, B.; Stein, A.; Lodge, T.P.; Hillmyer, M.A.; Bühlmann, P. Solid-Contact Ion-Selective and Reference Electrodes Covalently Attached to Functionalized Poly(ethylene terephthalate). *Anal. Chem.* **2020**, *92*, 7621–7629. [CrossRef]

8. Paut, A.; Prkic, A.; Mitar, I.; Boskovic, P.; Jozic, D.; Jakic, M.; Vukusic, T. Potentiometric Response of Solid-State Sensors Based on Ferric Phosphate for Iron(III) Determination. *Sensors* **2021**, *21*, 1612. [CrossRef]

9. Rousseau, C.R.; Bühlmann, P. Calibration-free potentiometric sensing with solid-contact ion-selective electrodes. *TrAC Trends Anal. Chem.* **2021**, *140*, 116277. [CrossRef]

10. Ivanko, I.; Lindfors, T.; Emanuelsson, R.; Sjödin, M. Conjugated redox polymer with poly(3,4-ethylenedioxythiophene) backbone and hydroquinone pendant groups as the solid contact in potassium-selective electrodes. *Sens. Actuators B Chem.* **2021**, *329*, 129231. [CrossRef]

11. Kamel, A.H.; Amr, A.E.-G.E.; Al-Omar, M.A.; Almehizia, A.A. Solid-State Membrane Sensors Based on Man-Tailored Biomimetic Receptors for Selective Recognition of Isoproturon and Diuron Herbicides. *Membranes* **2020**, *10*, 279. [CrossRef]

12. Cattrall, R.W.; Freiser, H. Coated wire ion-selective electrodes. *Anal. Chem.* **1971**, *13*, 1905–1906. [CrossRef]

13. Rostampour, M.; Bailey, B.; Autrey, C.; Ferrer, K.; Vantoorenburg, B.; Patel, P.K.; Calvo-Marzal, P.; Chumbimuni-Torres, K.Y. Single-Step Integration of Poly(3-Octylthiophene) and Single-Walled Carbon Nanotubes for Highly Reproducible Paper-Based Ion-Selective Electrodes. *Anal. Chem.* **2021**, *93*, 1271–1276. [CrossRef] [PubMed]

14. Bobacka, J.; Ivaska, A.; Lewenstam, A. Potentiometric Ion Sensors. *Chem. Rev.* **2008**, *108*, 329–351. [CrossRef]

15. Yu, K.; He, N.; Kumar, N.; Wang, N.; Bobacka, J.; Ivaska, A. Electrosynthesized polypyrrole/zeolite composites as solid contact in potassium ion-selective electrode. *Electrochim. Acta* **2017**, *228*, 66–75. [CrossRef]

16. Bobacka, J. Conducting Polymer-Based Solid-State Ion-Selective Electrodes. *Electroanalasys* **2006**, *18*, 7–18. [CrossRef]

17. Gadhari, N.S.; Gholave, J.V.; Patil, S.S.; Patil, V.R.; Upadhyay, S.S. Enantioselective high performance new solid contact ion-selective electrode potentiometric sensor based on sulphated γ-cyclodextrin-carbon nanofiber composite for determination of multichiral drug moxifloxacin. *J. Electroanal. Chem.* **2021**, *882*, 114981. [CrossRef]

18. Kraikaew, P.; Sailapu, S.K.; Bakker, E. Rapid Constant Potential Capacitive Measurements with Solid-Contact Ion-Selective Electrodes Coupled to Electronic Capacitor. *Anal. Chem.* **2020**, *92*, 14174–14180. [CrossRef] [PubMed]

19. Zeng, X.; Yu, S.; Yuan, Q.; Qin, W. Solid-contact K^+-selective electrode based on three-dimensional molybdenum sulfide nano-flowers as ion-to-electron transducer. *Sens. Actuators B Chem.* **2016**, *234*, 80–83. [CrossRef]

20. Rutkowska, M.; Lindfors, T.; Boeva, Z.; Strawski, M. Low-cost flexible laminated graphene paper solid-contact ion-selective electrodes. *Sens. Actuators B Chem.* **2021**, *337*, 129808. [CrossRef]

21. Li, J.; Qin, W. An integrated all-solid-state screen-printed potentiometric sensor based on a three-dimensional self-assembled graphene aerogel. *Microchem. J.* **2020**, *159*, 105453. [CrossRef]

22. Kozma, J.; Papp, S.; Gyurcsányi, R.E. Solid-contact ion-selective electrodes based on ferrocene-functionalized multi-walled carbon nanotubes. *Electrochem. Commun.* **2021**, *123*, 106903. [CrossRef]

23. Lenar, N.; Piech, R.; Paczosa-Bator, B. High Capacity Nanocomposite Layers Based on Nanoparticles of Carbon Materials and Ruthenium Dioxide for Potassium Sensitive Electrode. *Materials* **2021**, *14*, 1308. [CrossRef]

24. Lenar, N.; Piech, R.; Wyrwa, J.; Paczosa-Bator, B. Potassium-Selective Solid-Contact Electrode with High-Capacitance Hydrous Iridium Dioxide in the Transduction Layer. *Membranes* **2021**, *11*, 259. [CrossRef]

25. Mendoza-Sánchez, B.; Gogotsi, Y. Synthesis of Two-Dimensional Materials for Capacitive Energy Storage. *Adv. Mater.* **2016**, *28*, 6104–6135. [CrossRef]

26. Gan, X.; Zhao, H.; Quan, X. Two-dimensional MoS_2: A promising building block for biosensors. *Biosens. Bioelectron.* **2017**, *89*, 56–71. [CrossRef]

27. Wang, Q.; Jiao, L.; Du, H.; Wang, Y.; Yuan, H. Fe_3O_4 nanoparticles grown on graphene as advanced electrode materials for supercapacitors. *J. Power Sources* **2014**, *245*, 101–106. [CrossRef]

28. Yin, T.; Jiang, X.; Qin, W. A magnetic field-directed self-assembly solid contact for construction of an all-solid-state polymeric membrane Ca^{2+}-selective electrode. *Anal. Chim. Acta* **2017**, *989*, 15–20. [CrossRef]

29. Chen, Y.; Song, B.; Tang, X.; Lu, L.; Xue, J. Ultrasmall Fe_3O_4 Nanoparticle/MoS_2 Nanosheet Composites with Superior Performances for Lithium Ion Batteries. *Small* **2014**, *10*, 1536–1543. [CrossRef]

30. Chen, Y.; Song, B.; Lu, L.; Xue, J. Ultra-small Fe_3O_4 nanoparticle decorated graphene nanosheets with superior cyclic performance and rate capability. *Nanoscale* **2013**, *5*, 6797–6803. [CrossRef]

31. Liu, J.; Du, J.; Su, Y.; Zhao, H. A facile solvothermal synthesis of 3D magnetic MoS_2/Fe_3O_4 nanocomposites with enhanced peroxidase-mimicking activity and colorimetric detection of perfluorooctane sulfonate. *Microchem. J.* **2019**, *149*, 104091. [CrossRef]

32. Zeng, X.; Qin, W. A solid-contact potassium-selective electrode with MoO_2 microspheres as ion-to-electron transducer. *Anal. Chim. Acta* **2017**, *982*, 72–77. [CrossRef] [PubMed]

33. Shao, Y.; Ying, Y.; Ping, J. Recent advances in solid-contact ion-selective electrodes: Functional materials, transduction mechanisms, and development trends. *Chem. Soc. Rev.* **2020**, *49*, 4405–4465. [CrossRef]

34. Bobacka, J. Potential Stability of All-Solid-State Ion-Selective Electrodes Using Conducting Polymers as Ion-to-Electron Transducers. *Anal. Chem.* **1999**, *71*, 4932–4937. [CrossRef]

35. Crespo, G.A.; Macho, S.; Rius, F.X. Ion-Selective Electrodes Using Carbon Nanotubes as Ion-to-Electron Transducers. *Anal. Chem.* **2008**, *80*, 1316–1322. [CrossRef] [PubMed]

36. Zeng, X.; Qin, W. A solid-contact Ca^{2+}-selective electrode based on an inorganic redox buffer of Ag@AgCl/1-tetradecyl-3-methylimidazolium chloride as ion-to-electron transducer. *Talanta* **2020**, *209*, 120570. [CrossRef]

37. Fibbioli, M.; Morf, W.E.; Badertscher, M.; de Rooij, N.F.; Pretsch, E. Potential Drifts of Solid-Contacted Ion-Selective Electrodes Due to Zero-Current Ion Fluxes Through the Sensor Membrane. *Electroanalysis* **2010**, *12*, 1286–1292. [CrossRef]